BULETINUL INSTITUTULUI POLITEHNIC DIN IAŞI
Publicat de
Universitatea Tehnică „Gheorghe Asachi” din Iaşi
Volumul 63 (67), Numărul 4, 2017
Secţia
CONSTRUCŢII DE MAŞINI

INSTANTANEOUS ANGULAR SPEED MONITORING BASED ON SIGNAL AMPLITUDE OF AN AC GENERATOR USED AS SENSOR

BY

IONUŢ CIURDEA and MIHĂIŢĂ HORODINCĂ*

"Gheorghe Asachi" Technical University of Iaşi,
Faculty of Machine Manufacturing and Industrial Management

Received: October 16, 2017
Accepted for publication: December 19, 2017

Abstract. The paper presents some achievements in experimental approach on computer aided instantaneous angular speed (IAS) monitoring of mechanical rotating systems using an AC generator as sensor. A simple setup consists of a sensor, a numerical oscilloscope and a computer is necessary. The evolution of AC signal amplitude is used to define by calculus the evolution of IAS in time domain. The features of IAS in experimental research (monitoring and diagnosis of a rotary machine) are illustrated by computer aided signal processing in time and frequency domains during a simple experiment accomplished on IAS monitoring for the output shaft of a lathe headstock used as rotating machine.

Keywords: Instantaneous angular speed; AC generator; signal processing; monitoring; diagnosis.

1. Introduction

Actually the evolution of instantaneous angular speed (IAS) measured on a rotating shaft is an important issue and a big challenge in rotating machines condition investigation (Rémond *et al*., 2014). An appropriate computer-

*Corresponding author; *e-mail*: horodinca@tuiasi.ro

assisted study on IAS evolution and IAS signal contents revealed some important resources available in experimental research. There are some important advantages of monitoring based on IAS evolution:

– The IAS evolution is one of the most significant parameter directly involved in rotary machine condition monitoring and diagnosis (Renaudin *et al*., 2010; Li *et al*., 2012; Lei *et al*., 2014; Li *et al*., 2017);

– Many IAS sensors are available: rotary encoders (Bourdon *et al.*, 2014; Zhao *et al*., in press 2018), rotary resolvers (Sarma *et al*., 2008; Bourogaoui *et al*., 2016) or similar devices as variable reluctance sensors (Guo *et al*., 2017);

– There are many available techniques of IAS signal processing useful in time and frequency domains analysis, most of them inspired from vibration signal processing (Charchalis and Dereszewski, 2013; Li and Zhang, 2017; Guo *et al*., 2017).

Generally an IAS sample is the result of calculus by dividing a known angle with a variable time interval, measured with approximation by time elapsed method (Li *et al*., 2005). Despite the fact that the angle is not extremely small and the angular speed is in reality expressed as an average value, we propose to accept the angular speed as being instantaneous.

In order to avoid several shortcomings of usually IAS measurement techniques (*e.g*., a relative complicate sensor -frequently electrical supplied- and a difficult elapsed time measurement) some possible new contributions in the field were identified in this paper which is focussed on the exploitation of a single-phase *n* poles AC generator as sensor. The amplitude evolution of AC signal delivered by this sensor placed on a rotating shaft is used for IAS measurement, monitoring and signal content analysis. A brushless stepper motor plays the role of this generator. A simple computer assisted experimental setup was used. Some experiments and results prove the consistency of this approach.

In Section 2 of this paper a short theoretical approach is done, in Section 3 the experimental setup is depicted, Section 4 presents some experimental results comments and discussion, Section 5 is reserved for conclusions and future work.

2. IAS Measurement Based on AC Signal Features

According with Faraday law of electromagnetic induction, the instantaneous voltage $u(t)$ delivered by a single-phase n poles AC generator when its rotor rotates with the instantaneous angular speed ω is mathematically described by:

$$u(t) = U \sin(n \cdot \omega \cdot t) \tag{1}$$

The angular speed is involved in this definition in two ways:

– Firstly ω is placed inside the argument of sinus function. It has a direct influence on the signal period $T=2\pi/(n\cdot\omega)$ of the harmonic evolution from Eq. (1) or on semi-period $T_s=\pi/(n\cdot\omega)$ as well. On each rotation with an angular space of $2\cdot\pi/n$ there is a complete wave cycle on the signal $u(t)$ (a period T, or two semi-periods T_s as well). On each complete rotation of the rotor there are n complete wave cycles.

– Secondly ω is entailed in amplitude U definition, with a theoretically presumed proportional relationship between: $\omega=C\cdot U$ (suppose that the constant C is known).

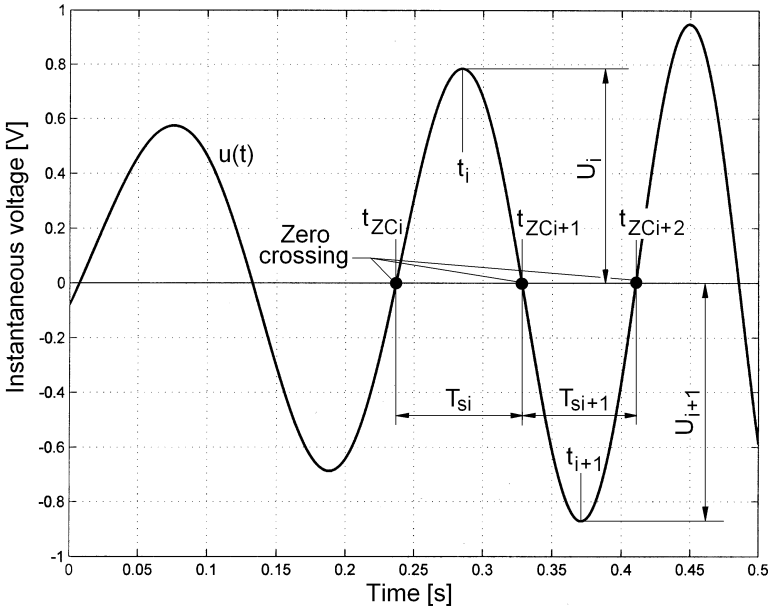

Fig. 1 – A numerical simulation of $u(t)$ with graphical depiction of the elements (T_{si} and U_i) involved in the definitions of generic sample ω_i of IAS.

Suppose that the IAS evolution is numerically described by a generic sample ω_i measured at sample time t_i. If the signal $u(t)$ is converted in numerical format (by analog to digital conversion) and acquired by a computer, each one of these two previous relationships allows an IAS different indirect measurement procedure. A first procedure (as IAST) is based on signal semi-period measurement and produces a generic sample:

$$\omega_{Ti}=\frac{\pi}{n\cdot T_{si}} \tag{2}$$

A second procedure (as IASA) is based on amplitude U_i measurement on each semi-period and produces a generic sample:

$$\omega_{Ai} = C \cdot U_i \tag{3}$$

If both procedures are used simultaneously (each two generic samples ω_{Ti}, ω_{Ai} should be equal) then C is theoretically available by calculus from Eqs. (2) and (3) as:

$$C = \frac{\omega_{Ti}}{U_i} = \frac{\pi}{U_i \cdot n \cdot T_{si}} \tag{4}$$

There is an important difference of IAS description in these two different procedures: an average value of IAS is calculated for each half wave cycle (semi-period) of $u(t)$ in IAST, an instantaneous value of IAS is calculated on each semi-period in IASA.

With ω slowly variable, on $u(t)$ evolution simulated in Fig. 1, a generic semi-period T_{si} is defined as the time elapsed between two successive generic zero-crossing moments $T_{si} = t_{ZCi+1} - t_{ZCi}$ and the generic amplitude U_i is the maximum value of $u(t)$ value between t_{ZCi} and t_{ZCi+1} moments on the positive part of $u(t)$ wave cycle, or the modulus of minimum value on the negative part of $u(t)$ wave cycle (*e.g.*, U_{i+1}). On a complete wave cycle there are two samples of IAST (or IASA) with a generic sample time t_i conventionally described as $t_i = (t_{ZCi} + t_{ZCi+1})/2$. This corresponds to a constant IAS sample rate of $2 \cdot n$ samples per rotation. If f_r is the frequency of rotation of generator rotor then a variable IAS sample rate of $R_\omega = 2 \cdot n \cdot f_r$ samples per second can be defined. In both situations the sampling time of IAS is $\Delta t_\omega = t_{i+1} - t_i \approx T_{si}$.

While IAST method suppose an accurate detection of zero-crossing moments of $u(t)$ signal (a relative complicate issue if the sampling rate of $u(t)$ is small), IASA method is efficient even with an approximate detection of these moments. This detection is done as follows: if t_{uj} and t_{uj+1} are two successive generic samples of $u(t)$ numerical description then an approximate generic zero-crossing moment detection is done (with $t_{ZCi} \approx t_{uj}$) if $u(t_{uj}) \cdot u(t_{uj+1}) < 0$ (the voltage of a generic sample $u(t)$ is positive and the next one is negative or vice versa) supposing that $u(t_{uj})$ and $u(t_{uj+1}) \neq 0$.

In this paper the research on IASA is privileged. For comparison purposes -at least for experimental determination of the constant C involved in Eq. (4)- an approximate IAST method ($IAST_{app}$) based on approximate detection zero-crossing moments -introduced previously- will be used. A future approach will be focussed on high accuracy IAST measurement method ($IAST_{acc}$) and accurate zero-crossing detection too.

Some computer assisted programs was written (in Matlab) and employed to solve the items indicated above (detection of zero-crossing moments, amplitudes and sample time on numerical signal $u(t)$, IASA calculus), numerical filtering of $u(t)$ and IASA, signal processing in time and frequency domains.

3. Experimental Setup

A big advantage of this approach is the simplicity of experimental setup. An experimental study proves that a two-phase stepper motor (Shinano Kenshi STH-56D101 with 200 steps per rotation) used as generator works properly as an IAS sensor (a single-phase *n* poles AC generator or variable reluctance sensor as well, with $n = 50$) if its rotor rotates at relative high angular speed. The AC signal delivered by a single phase of this generator can be directly converted in numerical format (via a numerical oscilloscope) and delivered to a computer. No need of additional electronic devices (for signal conditioning) or power supply for sensor. A partial view of the experimental setup is given in Fig. 2. Here are depicted the stepper motor and the numerical oscilloscope (PicoScope 4824 from Pico Technology UK, 12 bit resolution and selectable sensitivity).

Fig. 2 – A partially view on experimental setup components.

Some experiments of IAS monitoring were done with the sensor rotor firmly fasten on the output shaft of a Romanian SNA 360 lathe headstock (using a jaw chuck) turning in transient and stationary regimes. This setup is fully available for many other rotating machines or systems.

4. Experimental Results and Discussion

4.1. IASA and $IAST_{app}$ Experimental Evolutions in Time Domain

A first experimental approach is related with IAS evolutions with both methods ($IAST_{app}$ and IASA) described in Fig. 3 during a transient regime of lathe headstock consists of three different stages: acceleration (A_1), steady-state regime (A_2) with a relative constant IAS (109.25 rad/s average value) and free cessation of motion (A_3) after the actuation ceased. Here a more accurate way to calculate the constant *C* in IASA was applied if Eq. (4) is rewritten as:

$$C \cdot \frac{1}{N}\sum_{i=1}^{n} U_i = \frac{1}{N}\sum_{i=1}^{n} \omega_{Ti} \qquad C = \sum_{i=1}^{n} \omega_{Ti} / \sum_{i=1}^{n} U_i \tag{5}$$

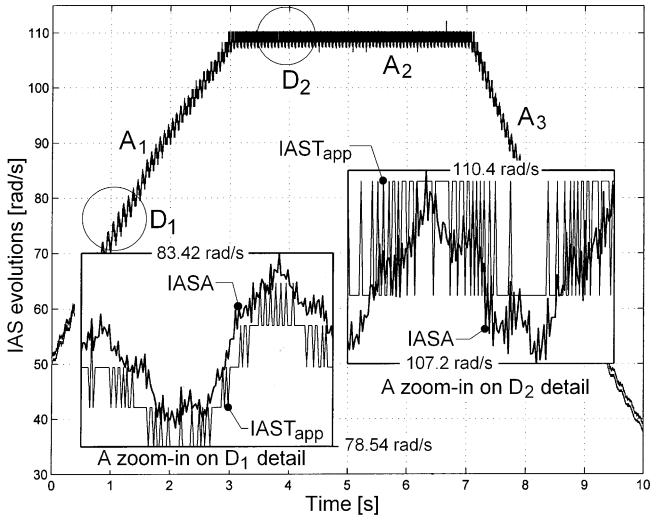

Fig. 3 – Experimental IAS evolutions ($IAST_{app}$ and IASA) on the output shaft lathe headstock in time domain (with proportional dependence between ω_{Ai} and U_i on IASA).

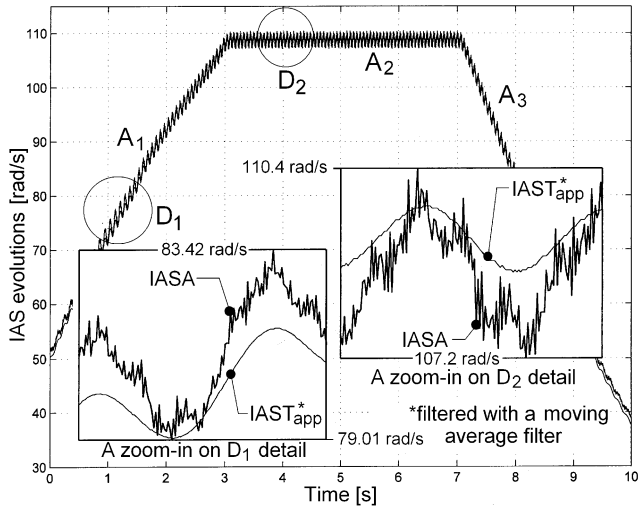

Fig. 4 – The evolutions from Fig. 3 with $IAST_{app}$ low-pass filtered.

Here C is the result of a ratio between the average value of amplitudes and average value of IAS. In Eq. (5) N is the number of IAS samples. In Fig. 3 there are 14.237 IAS samples. Eq. (5) generates a value C=3.9416 rad/V·s.

Fig. 3 presents two zoom-in details: D_1 on A_1 stage and D_2 on A_2 stage (0.1 s duration each one). On both details it is obvious that there are important differences between IASA and $IAST_{app}$ evolutions.

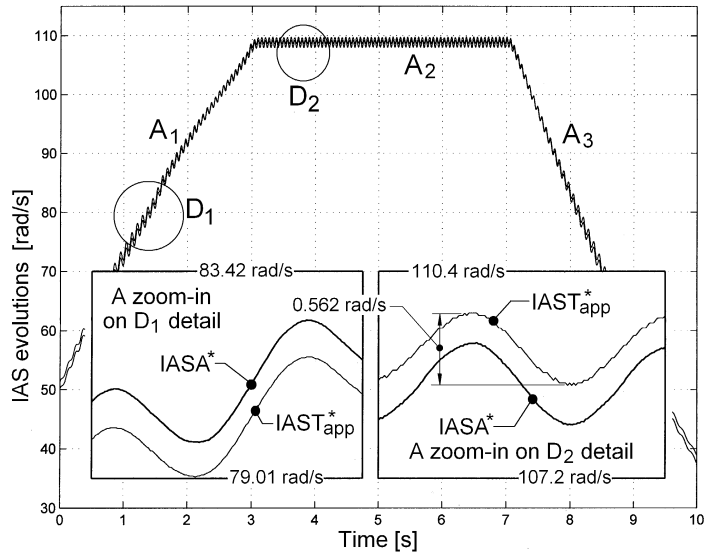

Fig. 5 – The evolutions from Fig. 3 with $IAST_{app}$ and IASA low-pass filtered (with a moving average filter).

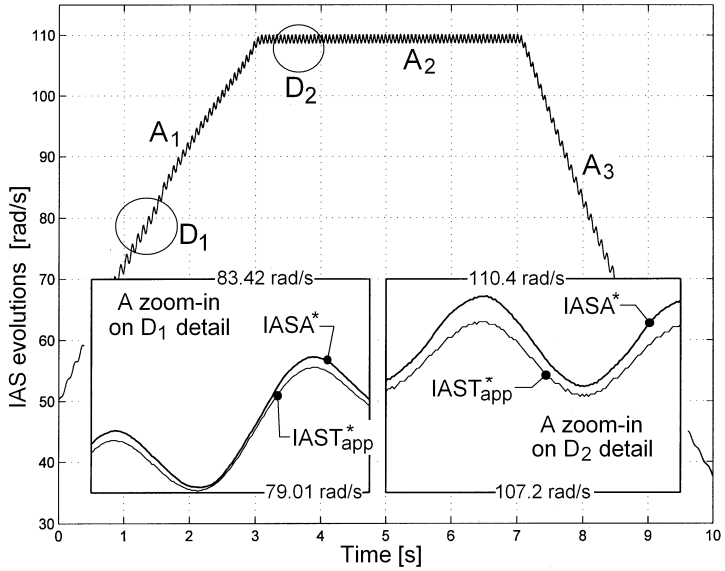

Fig. 6 – The evolutions from Fig. 5 with a parabolic dependence between ω_{Ti} and U_i on IASA depicted in Eq. (6).

Because the zero-crossing moments (and the semi-periods involved in Eq. (2) too) are not accurately described, the $IAST_{app}$ is affected by a huge quantization error (due to the quantization error of semi-period equal with sampling time of numerical description of $u(t)$). Because of these errors, some small variations of IAS are not revealed in $IAST_{app}$ evolution (as the zoom-in on D_1 and D_2 details indicate).

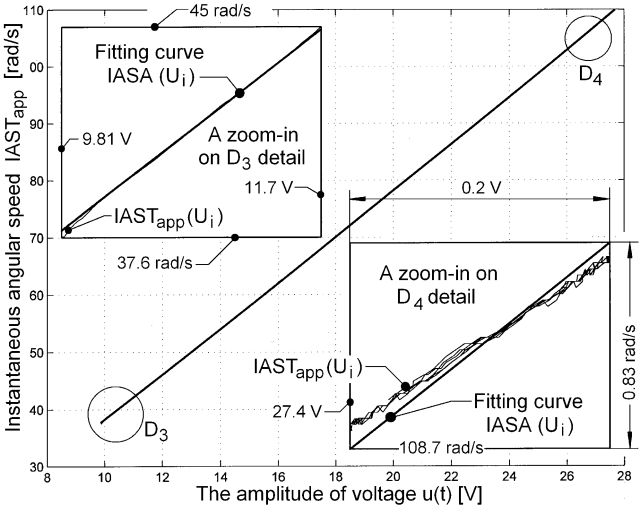

Fig. 7 – Graphical elements related to approximation of experimental evolution $\omega_{Ti}(U_i)$ with a parabola by curve fitting and zoom-in details.

However a significant part of this undesirable quantization error effect can be removed if the $IAST_{app}$ is numerically low pass filtered with a moving average filter (Ciurdea and Horodincă, 2017) with fifty samples in the average, as Fig. 4 indicates. Two observations are available here:

1. Both evolutions have a low frequency harmonic component with the frequency of rotation of the output shaft (no phase shift between). In contrast to the IASA evolution, the filtered $IAST_{app}$ evolution describes with accuracy only this low frequency variable component.

2. There is not a perfect overlay of average values of IASA and $IAST_{app}$ because there is not a strict proportionality between ω_{Ai} and U_i as presumed in Eq. (3), or C is not constant (the calculus with Eqs. (4) and (5) is an approximation). This is more clearly indicated on Fig. 5 (with IASA and $IAST_{app}$ filtered with the same type of low pass filter). The average IASA is bigger than average $IAST_{app}$ at low speed and smaller at high speed. This is a real disadvantage of IASA measurement method (in opposite, the average of filtered $IAST_{app}$ is not affected by significant errors). This deviation to the proportionality between ω_{Ai} and U_i is due to the fact that the stepper motor

doesn't work probably as an ideal AC generator. This inconvenience is partially eliminated (as Fig. 6 indicates) if the proportional dependence between the generic samples ω_{Ai} and U_i is replaced with a parabolic relationship:

$$\omega_{Ai} = 0.009261 \cdot U_i^2 + 3.700 \cdot U_i + 0.444858 \tag{6}$$

The parameters involved in Eq. (6) were determined by curve fitting (in Matlab) in order to find the theoretically parabola which ensures the best fitting with experimental evolution (ω_{Ti} versus U_i).

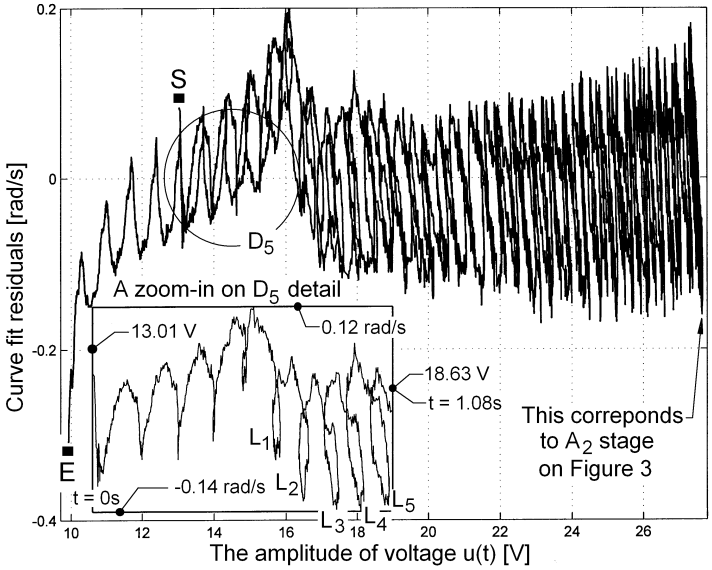

Fig. 8 – Graphical description of parabolic curve fit residuals (the generic difference ω_{Ti}-ω_{Ai} on ordinate versus U_i on abscissa).

Fig. 7 indicates some graphic elements of this curve fitting process. Apparently the theoretical and experimental evolutions fit well (the arc of parabola is very close by a line segment; see here below Eq. (7)). Practically still there are small differences between these evolutions as is revealed in D_1 and D_2 details on Fig. 6, in D_4 detail on Fig. 7 and in Fig. 8 which describes the curve fit residuals (the evolution of generic difference between measured filtered ω_{Ti} and calculated ω_{Ai} with Eq. (6) having in the abscissa the generic U_i). On Fig. 8 the curve fit residuals is roughly placed between – 0.2 and + 0.2 rad/s with periodical loops ($L_1 \div L_5$ revealed in D_5 detail, with a 1000 samples) and different path from the start point of evolution (S, for t = 0) to the endpoint (E, for t = 10 s). These loops and path differences are related probably to a delay in mirroring of variable phenomena in $IAST_{app}$ and IASA and to the averaging process.

It is also possible to use a linear dependence to approximate the experimental evolution (ω_{Ti} versus U_i), determined also by curve fitting as:

$$\omega_{Ai} = 4.08 \cdot U_i - 3.075 \tag{7}$$

As Fig. 9 indicates, now the approximation is worse than before, the residuals is placed between – 0.5 and + 0.5 rad/s. The shape of the residual is close by a parabola, this being a good argument for parabolic curve fitting described above.

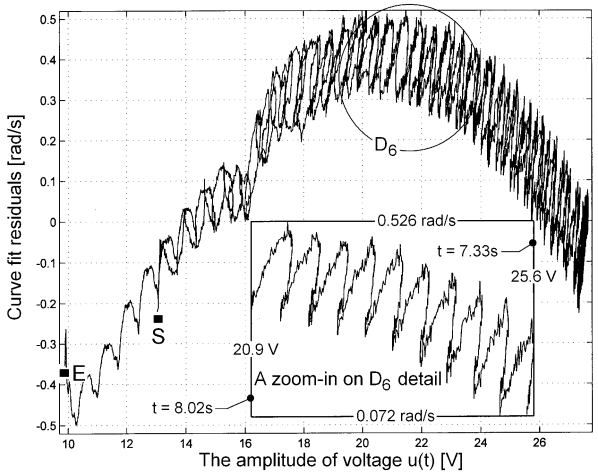

Fig. 9 – Graphical description of linear curve fit residuals (the generic difference ω_{Ti}-ω_{Ai} on ordinate versus U_i on abscissa).

Despite the relative small accuracy, the IASA monitoring procedure is a promising issue, especially because it has a better capability of description for high frequency variable components (by comparison with $IAST_{app}$), revealed in next section of this paper.

4.2. $IAST_{app}$ and IASA Experimental Evolutions in Frequency Domain

The IAS evolution in steady-state regime (*e.g.*, sequence A_2 on Fig. 3) is useful for a well known signal analysis procedure: the conversions of evolution from time domain to frequency domain by fast Fourier transform (FFT). This procedure is able, for diagnosis purposes, to detect and to describe the harmonic components (the values of frequency and amplitude) induced by different parts inside a mechanical system (a lathe headstock here) due to a normal operation or (most frequently) due to a malfunctioning (tolerable or non-tolerable). A simple computer program written in Matlab was used to provide the FFT. A first approach from Fig. 10 presents the FFT of $IAST_{app}$ signal for A_2 sequence.

The Nyquist frequency f_N (the maximum available frequency in the spectrum) is the half of sampling rate $f_N = R_\omega/2 = n \cdot f_r$ = 50·17.387 Hz = 869.35 Hz (for an average value 17.387 Hz of rotation frequency). As expected, only a small part of spectrum (depicted in D_7 detail, roughly from 0 to 100 Hz) contains a relative good description of the harmonic components. Here of course the dominant peak (0.795 rad/s amplitude, already revealed on D_2 detail on Fig. 5 having 0.562 rad/s amplitude because of filtering) is related to the rotation frequency f_r.

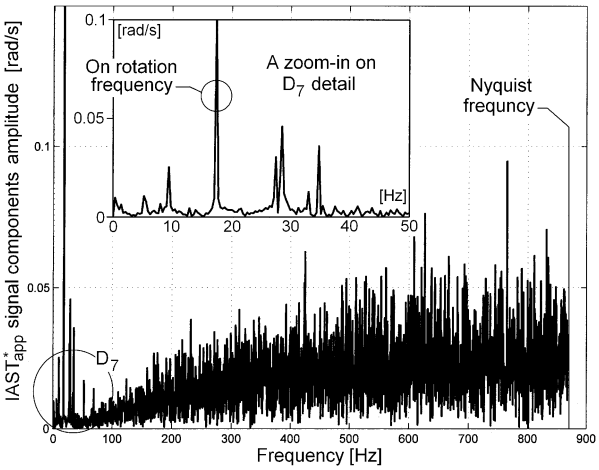

Fig. 10 – The evolution of $IAST_{app}$ (on A_2 sequence from Fig. 3) in frequency domain by FFT.

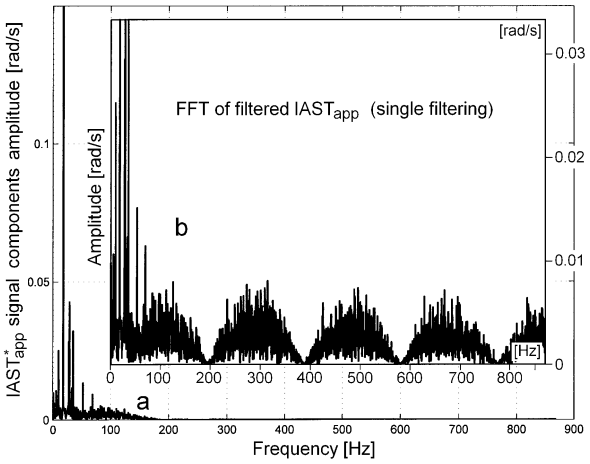

Fig. 11 – The evolution of filtered $IFFT_{app}$ (on A_2 sequence from Fig. 3) in frequency domain by FFT; a) filtered with a multiple average filter; b) filtered with a single average filter (magnification of 3x).

All other peaks from D_7 detail are related with periodical phenomena inside the lathe headstock. As a big disadvantage of $IAST_{app}$ the remaining part of the spectrum (from 100 Hz up to f_N) is not useful for diagnosis, as being generated only by the quantization errors (having a big amount of noise). Of course on the FFT of numerical filtered $IAST_{app}$ with a multiple (repetitive) average filter (Ciurdea and Horodincă, 2017) this part of spectrum completely disappears, as Fig. 11*a*) indicates (after 200 Hz). This numerical filtering is done with these Matlab instructions:

```
tur=smooth(tur,10);tur=smooth(tur,8);
tur=smooth(tur,5);tur=smooth(tur,3);
```

with progressively decreasing number of samples in the average.

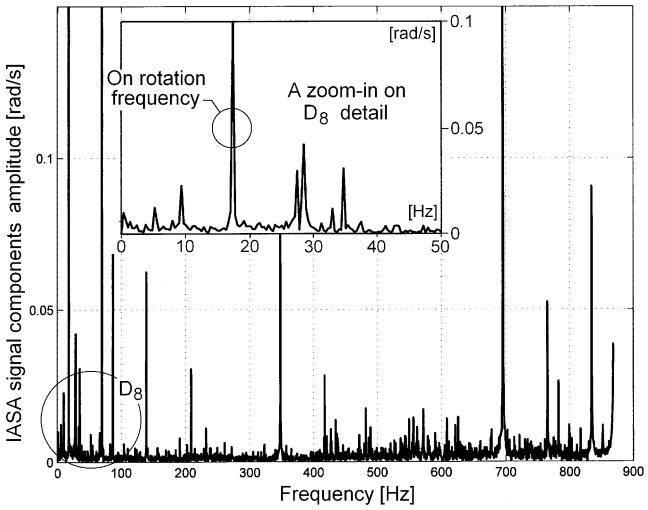

Fig. 12 – The evolution of IASA (on A_2 sequence from Fig. 3) in frequency domain by FFT.

Fig. 11*b* presents the FFT of $IAST_{app}$ (magnification of 3x) filtered with a single filter (`tur=smooth(tur,10)`. Here the spectrum content with lobes on high frequencies is due to the filter transmissibility (Ciurdea and Horodincă, 2017).

In contrast with the results from Fig. 10 (FFT of $IAST_{app}$) the FFT of IASA for the same sequence A_2 looks different, as Fig. 12 indicates. The entire spectrum is available with some distinct signal components (peaks) and low level of noise. Each one of these distinct components describes the behaviour of a rotary part inside the lathe headstock (as fundamentals and harmonic correlated components) or torsional vibration modes allowing the condition diagnosis (a privileged topic for a future research).

Nevertheless it is important to highlight that at low frequency the spectra of $IAST_{app}$ and IASA are almost identical, as it is revealed on the details D_7 (on Fig. 11) and D_8 (on Fig. 12). In order to make the comparison easier, in

Fig. 13 these details are depicted simultaneously. The evolution of IASA is moved up with 0.04 rad/s. There is a difference between the main components on spectra (on rotation frequency) with 0.795 rad/s amplitude on $IAST_{app}$ and 0.922 rad/s on IASA. The presence of this main component indicates that the rotation frequency is not constant (as already was revealed on D_2 details of Figs. 3 ÷ 6).

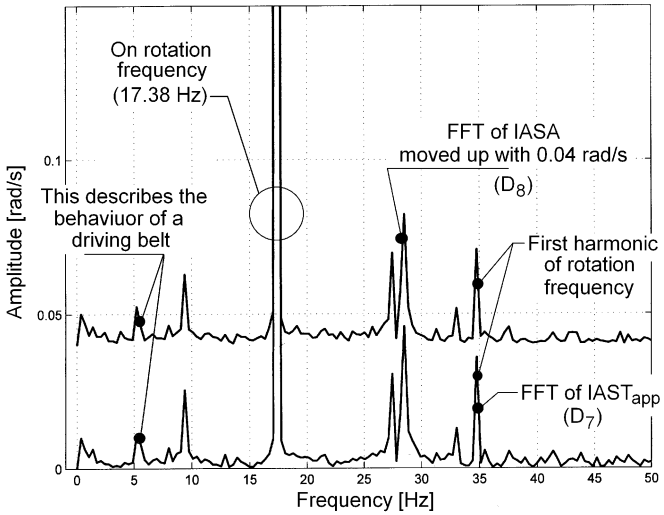

Fig. 13 – The evolution of IASA and $IAST_{app}$ in frequency domains (from details D_7 and D_8). The evolution of IASA is moved up with 0.04 rad/s.

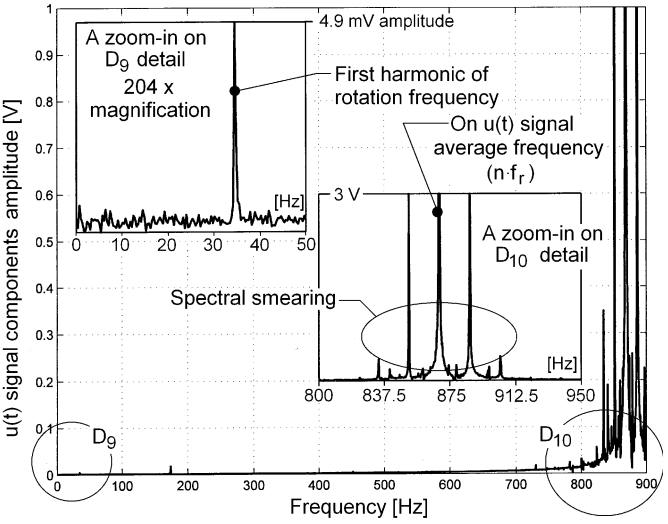

Fig. 14 – The evolution of $u(t)$ in frequency domain (on A_2 sequence from Fig. 3).

A periodical mechanical loading is introduced by the rotation of output shaft (probably due to the bearings) so a periodical variation of IAS is generated (due to the negative slope of dependence between mechanical loading and IAS).

Apparently the signal $u(t)$ delivered by the AC generator should be also useful directly for monitoring and diagnosis in frequency domain. If the supposition is true then these experimental research issues becomes much simpler: no need to convert previously the signal $u(t)$ in IASA.

Unfortunately this supposition is not true, as it is proved in Fig. 14 which shows the spectrum of $u(t)$ signal in the frequency domain used in Fig. 12. The only significant components occurs around the frequency of $u(t)$ signal ($n \cdot f_r$) due to the so called spectral smearing (Stander and Heyns, 2005) revealed on D_{10} detail. This spectral smearing is a result of FFT procedure in Matlab because the rotation frequency is not constant.

In the detail D_{10} the dominant component has 25.15 V amplitude and 869 Hz frequency. In D_9 detail is depicted the magnified spectrum (204x) between 0 and 50 Hz. It looks totally different by comparison with the details D_7 and D_8 (Figs. 10 and 12). As a curiosity, here occurs only a description of first harmonic component of rotation frequency.

5. Conclusions and Future Work

The paper illustrates some theoretical and experimental research approaches related with IAS monitoring on rotating mechanical systems and machines. An *n*-poles AC generator used as sensor allows the usage of two different IAS monitoring methods: first ($IAST_{app}$ less accurate) is based on approximate AC signal semi-period measurement, second (IASA, more accurate) is based on AC signal amplitude measurement. A simple experimental setup (consists of a lathe headstock as mechanical system, a brushless stepper motor playing the role of AC generator with 50 poles, a numerical oscilloscope and a computer) and some signal processing techniques assure the approach on monitoring and diagnosis based on IAS measurement and evolution in time and frequency domains. Two IAS values are available on each complete wave cycle of AC signal (there are *n* cycles on each rotation). Some features of IASA analysis in frequency domains useful in computer aided diagnosis were revealed.

A future approach will be focused on analysis of IASA evolution in frequency domain in order to give an explanation (for diagnosis purposes) on the origin of all variable components in the spectrum (*e.g.*, for the spectrum from Fig. 12). A complete identification for fundamental and harmonics of these variable components (in order to find out the accurate values of amplitude, frequency and phase-shift related to origin of time) will be done.

In the future it is expected that the finding of a new procedure of accurate evaluation of AC signal semi-period will be a real benefit in defining an accurate IAS measurement method (as $IAST_{acc}$) expected to be better than

IASA. Also a study on increasing of IAS sampling rate (and Nyquist frequency or maximum value of frequency on spectrum as well) will be done.

Acknowledgements. This paper employed some experimental resources of Developing a Research Platform for Efficient and Sustainable Energy (ENERED) Grant, POSCCE-A2-02.2.1-2009-4 ID 911, implemented at "Gheorghe Asachi" Technical University of Iași, Romania, funded by European Social Fund and Romanian Research Authority.

REFERENCES

Bourdon A., André H., Rémond D., *Introducing Angularly Periodic Disturbances in Dynamic Models of Rotating Systems under Non-Stationary Conditions*, Mech. Syst. Signal. Process., **44**, 60-71 (2014).

Bourogaoui M., Sethom H.B.A., Belkhodja I.S., *Speed/Position Sensor Fault Tolerant Control in Adjustable Speed Drives – A Review*, ISA Transactions, **64**, 269-284 (2016).

Charchalis M., Dereszewski M., *Processing of Instantaneous Angular Speed Signal for Detection of a Diesel Engine Failure*, Math. Probl. Eng., 1-7 (2013).

Ciurdea I., Horodincă M., *Instantaneous Angular Speed Measurement and Signal Processing: A Brief Review*, Bul. Inst. Polit. Iaşi, s. Machine Construction, **63(67)**, *1*, 51-73 (2017).

Guo Y., Li W., Yu S., Han X., Yuan Y., Wang Z., Ma X., *Diesel Engine Torsional Vibration Control Coupling with Speed Control System*, Mech. Syst. Signal. Process., **94**, 1-13 (2017).

Lei Y., Lin J., Zuo M., He Z., *Condition Monitoring and Fault Diagnosis of Planetary Gearboxes: A Review*, Measurement, **48**, 292-305 (2014).

Li B., Zhang X., *A New Strategy of Instantaneous Angular Speed Extraction and its Application to Multistage Gearbox Fault Diagnosis*, J. Sound. Vib., **396**, 340-355 (2017).

Li B., Zhang X., Wu J., *New Procedure for Gear Fault Detection and Diagnosis Using Instantaneous Angular Speed*, Mech. Syst. Signal. Process., **85**, 415-428 (2017).

Li Y., Gu F., Harris G., Ball A., Bennett N., Travis K., *The Measurement of Instantaneous Angular Speed*, Mech. Syst. Signal. Process., **19**, 786-805 (2005).

Li Z., Yan X., Yuan C., Peng Z., *Intelligent Fault Diagnosis Method for Marine Diesel Engines Using Instantaneous Angular Speed*, J. Mech. Sci. Technol., **26**, *8*, 2413-2423 (2012).

Rémond D., Antoni J., Randall R.B., *Editorial for the Special Issue on Instantaneous Angular Speed (IAS) Processing and Angular Applications*, Mech. Syst. Signal. Process., **44**, 1-4 (2014).

Renaudin L., Bonnardot F., Musy O., Doray J.B., Rémond D., *Natural Roller Bearing Fault Detection by Angular Measurement of True Instantaneous Angular Speed*, Mech. Syst. Signal. Process., **24**, 1998-2011 (2010).

Sarma S., Agrawal V.K., Udupa S., Parameswaran K., *Instantaneous Angular Position and Speed Measurement Using a DSP Based Resolver-to-Digital Converter*, Measurement, **41**, 788-796 (2008).

Stander C.J., Heyns P.S., *Instantaneous Angular Speed Monitoring of Gearboxes under Non-Cyclic Stationary Load Conditions*, Mech. Syst. Signal. Process., **19**, 817-835 (2005).

Zhao M., Jia X., Lin J., Lei Y., Lee J., *Instantaneous Speed Jitter Detection via Encoder Signal and its Application for the Diagnosis of Planetary Gearbox*, Mech. Syst. Signal. Process., **98**, 16-31 (in press 2018).

MONITORIZAREA VITEZEI UNGHIULARE INSTANTANEE PE BAZA AMPLITUDINII SEMNALULUI FURNIZAT DE UN GENERATOR DE TENSIUNE ALTERNATIVĂ FOLOSIT CA SENZOR

(Rezumat)

Lucrarea prezintă unele consideraţii şi rezultate legate de cercetarea experimentală asistată de calculator a evoluţiei vitezei unghiulare instantanee (VUI) a sistemelor mecanice cu mişcare de rotaţie folosind un generator de tensiune alternativă ca traductor de VUI. Se foloseşte un stand experimental simplu ce include traductorul, un osciloscop numeric şi un calculator. Evoluţia amplitudinii tensiunii este folosită pentru determinarea prin calcul a evoluţiei temporale a semnalului de descriere a VUI. Facilităţile oferite de VUI în cercetarea experimentală (monitorizare şi diagnoză) sunt exemplificate prin procesarea semnalului în domeniile timp şi frecvenţă în legătură cu un simplu experiment de montorizare a vitezei unghiulare a arborelui de ieşire din cutia de viteze a unui strung folosit ca sistem mecanic cu mişcare de rotaţie.